

# IMPLEMENTATION OF MIXED METHODS AS FINITE DIFFERENCE METHODS AND APPLICATIONS TO NONISOTHERMAL MULTIPHASE FLOW IN POROUS MEDIA \*

Zhang-xin Chen

(Center for Scientific Computation, Box 750156, Southern Methodist University, Dallas, TX 75275-0156, USA)

(Research Center for Science, Xi'an Jiaotong University, Xi'an 710049, China)

(Center for Advanced Reservoir Modeling and Simulation, College of Engineering, Peking University, China)

Xi-jun Yu

(Laboratory of Computational Physics, Institute of Applied Physics and Computational Mathematics, Beijing 100088, China)

Dedicated to the 70th birthday of Professor Lin Qun

## Abstract

In this paper we consider mixed finite element methods for second order elliptic problems. In the case of the lowest order Brezzi-Douglas-Marini elements (if  $d = 2$ ) or Brezzi-Douglas-Durán-Fortin elements (if  $d = 3$ ) on rectangular parallelepipeds, we show that the mixed method system, by incorporating certain quadrature rules, can be written as a simple, cell-centered finite difference method. This leads to the solution of a sparse, positive semidefinite linear system for the scalar unknown. For a diagonal tensor coefficient, the sparsity pattern for the scalar unknown is a five point stencil if  $d = 2$ , and seven if  $d = 3$ . For a general tensor coefficient, it is a nine point stencil, and nineteen, respectively. Applications of the mixed method implementation as finite differences to nonisothermal multiphase, multicomponent flow in porous media are presented.

*Mathematics subject classification:* 65N30, 65N22, 76S05, 76T05.

*Key words:* Finite difference, Implementation, Mixed method, Error estimates, Superconvergence, Tensor coefficient, Nonisothermal multiphase, Multicomponent flow, Porous media.

## 1. Introduction

We consider mixed finite element approximations of the model elliptic problem

$$\begin{aligned} -\nabla \cdot (K\nabla p) &= f && \text{in } \Omega, \\ K\nabla p \cdot \nu &= 0 && \text{on } \partial\Omega, \end{aligned} \tag{1.1}$$

where  $\Omega$  is a domain in  $\mathbb{R}^d$ ,  $d = 2$  or  $3$ ,  $K$  is a symmetric, positive definite tensor with components in  $L^\infty(\Omega)$ ,  $\nu$  is the outer unit normal to the domain, and  $f$  satisfies the compatibility condition  $(f, 1) = 0$  (let  $(\cdot, \cdot)_S$  denote the  $L^2(S)$  inner product; we omit  $S$  if  $S = \Omega$ ). In applications to flow in porous media,  $p$  is the pressure,  $u = -K\nabla p$  is the velocity field, and  $K$  is the permeability tensor.

---

\* Received March 1, 2006.

Problem (1.1) is recast in mixed form as follows: Let

$$\begin{aligned} H(\operatorname{div}; \Omega) &= \{v \in (L^2(\Omega))^d : \nabla \cdot v \in L^2(\Omega)\}, \\ V &= \{v \in H(\operatorname{div}; \Omega) : v \cdot \nu = 0 \text{ on } \partial\Omega\}, \\ W &= L^2(\Omega). \end{aligned}$$

Then the mixed form of (1.1) for the pair  $(u, p) \in V \times W$  is

$$\begin{aligned} (\nabla \cdot u, q) &= (f, q), & \forall q \in W, \\ (K^{-1}u, v) - (p, \nabla \cdot v) &= 0, & \forall v \in V. \end{aligned} \tag{1.2}$$

To define a finite element method, we need a partition  $\mathcal{E}_h$  of  $\Omega$  into elements  $E$ , say, simplexes, rectangular parallelepipeds, and/or prisms, where adjacent elements completely share their common edge or face. Let  $V_h \times W_h \subset V \times W$  denote some standard mixed finite element space for second order elliptic problems defined over  $\mathcal{E}_h$  (see, e.g., [5, 6, 7, 13, 16, 18]). Then the mixed finite element solution of (1.2) is  $(u_h, p_h) \in V_h \times W_h$  satisfying

$$\begin{aligned} (\nabla \cdot u_h, q) &= (f, q), & \forall q \in W_h, \\ (K^{-1}u_h, v) - (p_h, \nabla \cdot v) &= 0, & \forall v \in V_h. \end{aligned} \tag{1.3}$$

The mixed method (1.3) requires the solution of a linear system in the form of a saddle point problem, which can be expensive to solve. An alternate approach was suggested by means of a nonmixed formulation. Namely, it is shown that the mixed finite element method is equivalent to a modification of the nonconforming Galerkin method [1, 3, 8, 12, 15]. The nonconforming method yields a symmetric and positive definite problem (i.e., a minimization problem). In the case that  $K$  is a diagonal tensor and one uses the lowest order Raviart-Thomas-Nédélec [16, 18] spaces over a rectangular grid, it is shown [19] that the linear system arising from the mixed formulation can be simplified by use of certain quadrature rules. That is, the mixed method system can be written as a cell-centered finite difference method.

An analogous simplification of the mixed method system as a finite difference method for another widely used space, the lowest order Brezzi-Douglas-Marini space [7] if  $d = 2$  or the lowest order Brezzi-Douglas-Durán-Fortin [5] space if  $d = 3$  has not been known. The objective of this paper is to derive a finite difference method for this space, without any loss in the rate of convergence, and retaining the superconvergence result. In particular, we show that for a diagonal tensor coefficient, the lowest order Brezzi-Douglas-Marini mixed method can be written as a cell-centered finite difference method with a five point stencil, and the Brezzi-Douglas-Durán-Fortin method can be given with a nine point stencil. For a general tensor coefficient, these two methods can be written with a nine point stencil, and nineteen, respectively. Our approach illuminates a relationship between the lowest order Raviart-Thomas-Nédélec and Brezzi-Douglas-Marini (or Brezzi-Douglas-Durán-Fortin) spaces; i.e., they can be written as the same finite difference method for the pressure by an appropriate use of quadrature rules.

The rest of the paper is organized as follows. In §2, we rewrite (1.2) using numerical quadrature rules for the evaluation of the integrals on each element  $E \in \mathcal{E}_h$ , and prove solvability. Then, in §3 we derive the finite difference method for the Brezzi-Douglas-Marini and Brezzi-Douglas-Durán-Fortin spaces. In §4, we mention some convergence and superconvergence results. In §5, we address another difficulty that the permeability  $K$  can be in practice zero in a subset of  $\Omega$ . We consider an expanded mixed formulation in the sense that three variables are explicitly treated, i.e., the pressure, the velocity field, and the flux field. This new formulation can handle the difficulty arising from the zero permeability [2, 9, 10, 11]. Finally, applications of the mixed method implementation as finite differences to nonisothermal multiphase, multicomponent flow in porous media are presented.

## 2. The Mixed Finite Element Method

The space  $V_h \times W_h$  is finite dimensional and defined locally on each element  $E \in \mathcal{E}_h$ , so let  $V_h(E) = V_h|_E$  and  $W_h(E) = W_h|_E$ . The constraint  $V_h \subset V$  says that the normal components of the members of  $V_h$  are continuous across the interior boundaries in  $\mathcal{E}_h$ . Recall that the lowest order Brezzi-Douglas-Marini space on rectangles is defined as

$$\begin{aligned} V_h(E) &= (P_1(E))^2 \oplus \text{span}\{\text{curl } x^2y, \text{curl } xy^2\}, \\ W_h(E) &= P_0(E). \end{aligned}$$

The Brezzi-Douglas-Durán-Fortin space on rectangular parallelepipeds is given by

$$\begin{aligned} V_h(E) &= (P_1(E))^3 \oplus \text{span}\{\text{curl}(0, 0, x^2y), \text{curl}(0, xz^2, 0), \text{curl}(y^2z, 0, 0), \\ &\quad \text{curl}(0, 0, xy^2), \text{curl}(0, x^2z, 0), \text{curl}(yz^2, 0, 0)\}, \\ W_h(E) &= P_0(E). \end{aligned}$$

We express approximately  $u_h$  in terms of  $p_h$  from the second equation of (1.3); then the first equation of (1.3) gives an equation for the pressure  $p_h$ . For this, we use numerical quadrature rules for the evaluation of the integrals in (1.3) on each element  $E \in \mathcal{E}_h$ . Throughout this paper,  $(\cdot, \cdot)_T$  represents an application of the midpoint rule. For the two-dimensional case,  $(\cdot, \cdot)_M$  denotes the numerical formula of an integral by applying the two-point Gaussian quadrature rule for the  $x$ -component over the vertical edges and for the  $y$ -component over the horizontal edges; for the three-dimensional case, we compute an integral by applying the four-point Gaussian quadrature rule for each component over its corresponding face. For a subdomain  $S$  of  $\Omega$ , we use the corresponding notation  $(u, v)_{S,T}$  and  $(u, v)_{S,M}$ . This choice of quadrature rules is compatible with the nodal basis functions for  $V_h$ . This technique is sometimes called a lumped mass approximation.

We now introduce the modified method for  $(u_h, p_h) \in V_h \times W_h$  satisfying

$$\begin{aligned} (\nabla \cdot u_h, q) &= (f, q)_T, & \forall q \in W_h, \\ (K^{-1}u_h, v)_M - (p_h, \nabla \cdot v) &= 0, & \forall v \in V_h. \end{aligned} \tag{2.1}$$

**Lemma 1.** *The system (2.1) has a unique solution.*

*Proof.* Since (2.1) is a finite dimensional, square, linear system, existence follows from uniqueness. To show uniqueness, let  $f = 0$ ,  $q = p_h$ , and  $v = u_h$ . Then the two equations in (2.1) imply that

$$(K^{-1}u_h, u_h)_M = 0.$$

Since  $K$  is symmetric and positive definite, this equation means that  $u_h$  vanishes at the two Gaussian points of the edges of each element. Hence  $u_h = 0$  everywhere. Since  $\nabla \cdot V_h = W_h$ , the second equation of (2.1) implies that  $p_h = 0$ .

## 3. Derivation of the Finite Difference Method

We present the derivation only for the case where  $d = 2$  and  $K = \text{diag}(K_1, K_2)$  is diagonal; the derivation for the three dimensional and full tensor cases is the same. Let  $\mathcal{E}_h \equiv \{x_{i+1/2}\}_{i=0}^{n_x} \times$

$\{y_{j+1/2}\}_{j=0}^{n_y}$  be a partition of  $\Omega$  and define

$$\begin{aligned} x_i &= \frac{1}{2}(x_{i+1/2} + x_{i-1/2}), & i &= 1, \dots, n_x, \\ y_j &= \frac{1}{2}(y_{j+1/2} + y_{j-1/2}), & j &= 1, \dots, n_y, \\ \Delta x_i &= x_{i+1/2} - x_{i-1/2}, \\ \Delta y_j &= y_{j+1/2} - y_{j-1/2}, \\ I_i^x &= (x_{i-1/2}, x_{i+1/2}), \\ I_j^y &= (y_{j-1/2}, y_{j+1/2}). \end{aligned}$$

For any function  $g(x, y)$ , let  $g_{i,j}$  denote  $g(x_i, y_j)$ , let  $g_{i+1/2,j}$  denote  $g(x_{i+1/2}, y_j)$ , and let  $g_{i,j+1/2}$  denote  $g(x_i, y_{j+1/2})$ .

From the definition of  $V_h(E)$  with  $E = I_i^x \times I_j^y$ , any element in  $V_h(E)$  has the form

$$v = (a + bx + cy + rx^2 + 2sxy, a_1 + b_1x + c_1y - 2rxy - sy^2), \quad (3.1)$$

where  $a \in \mathbb{R}$ , etc. Choose  $q = 1$  on  $E$  and equal to zero elsewhere in the first equation of (2.1) to obtain

$$(\nabla \cdot u_h, 1)_E = (f, 1)_{E,T}.$$

Then, by (3.1), we have

$$\{u_{i+1/2,j}^x - u_{i-1/2,j}^x\} \Delta y_j + \{u_{i,j+1/2}^y - u_{i,j-1/2}^y\} \Delta x_i = f_{i,j} \Delta x_i \Delta y_j, \quad (3.2)$$

where we used  $u^x$  to denote  $u_h^x$ , etc. To express  $u_h$  in terms of  $p_h$  from the second equation of (2.1), we now write the basis functions in  $V_h$ . To specify the constants in (3.1), we use the normal components of  $v$  at the two quadratic Gauss points on each edge of  $E$ . Then the basis function  $v_{i+1/2,j+}$  at the nodal point  $(x_{i+1/2}, y_j + \frac{\Delta y_j}{2\sqrt{3}})$  is

$$v_{i+1/2,j+} = (a + bx + cy + 2sxy, a_1 + c_1y - sy^2), \quad (3.3)$$

where, restricted to  $I_i^x \times I_j^y$ ,

$$\begin{aligned} a &= 2s(y_j - \frac{\Delta y_j}{2\sqrt{3}})x_{i-1/2}, \\ b &= -2s(y_j - \frac{\Delta y_j}{2\sqrt{3}}), \\ c &= -2sx_{i-1/2}, \\ a_1 &= -sy_{j-1/2}y_{j+1/2}, \\ c_1 &= 2sy_j, \\ s &= \frac{\sqrt{3}}{2\Delta x_i \Delta y_j}, \end{aligned} \quad (3.4)$$

restricted to  $I_{i+1}^x \times I_j^y$ ,

$$\begin{aligned} a &= 2s(y_j - \frac{\Delta y_j}{2\sqrt{3}})x_{i+3/2}, \\ b &= -2s(y_j - \frac{\Delta y_j}{2\sqrt{3}}), \\ c &= -2sx_{i+3/2}, \\ a_1 &= -sy_{j-1/2}y_{j+1/2}, \\ c_1 &= 2sy_j, \\ s &= -\frac{\sqrt{3}}{2\Delta x_{i+1} \Delta y_j}, \end{aligned} \quad (3.5)$$

and they are zero elsewhere.

Note that, by (3.4) and (3.5),

$$\begin{aligned} \left(p_h, \frac{\partial v_{i+1/2,j^+}^x}{\partial x}\right) &= (p_h, b + 2sy)_{I_i^x \times I_j^y} + (p_h, b + 2sy)_{I_{i+1}^x \times I_j^y} \\ &= \frac{1}{2}(p_{i,j} - p_{i+1,j})\Delta y_j, \end{aligned} \quad (3.6a)$$

and

$$\left(p_h, \frac{\partial v_{i+1/2,j^+}^y}{\partial y}\right) = (p_h, c_1 - 2sy)_{I_i^x \times I_j^y} + (p_h, c_1 - 2sy)_{I_{i+1}^x \times I_j^y} = 0. \quad (3.6b)$$

Next, exploit the same argument to see that

$$(K_1^{-1}u^x, v_{i+1/2,j^+}^x)_M = \frac{1}{2}\Delta y_j (K_1^{-1})_{i+1/2,j^+} u_{i+1/2,j^+}^x \frac{\Delta x_i + \Delta x_{i+1}}{2}, \quad (3.7a)$$

and

$$(K_2^{-1}u^y, v_{i+1/2,j^+}^y)_M = 0. \quad (3.7b)$$

Hence it follows from the second equation of (2.1), (3.6), and (3.7) that

$$u_{i+1/2,j^+}^x = -(K_1)_{i+1/2,j^+} \frac{p_{i+1,j} - p_{i,j}}{\Delta x_{i+1/2}}, \quad (3.8)$$

where  $\Delta x_{i+1/2} = (\Delta x_i + \Delta x_{i+1})/2$ . Analogously, we see that

$$u_{i+1/2,j^-}^x = -(K_1)_{i+1/2,j^-} \frac{p_{i+1,j} - p_{i,j}}{\Delta x_{i+1/2}}, \quad (3.9)$$

where  $u_{i+1/2,j^-}^x$  denotes the value of  $u^x$  at the point  $(x_{i+1/2}, y_j - \frac{\Delta y_j}{2\sqrt{3}})$ . Since

$$u_{i+1/2,j}^x = \frac{1}{2} \left( u_{i+1/2,j^+}^x + u_{i+1/2,j^-}^x \right),$$

we get

$$u_{i+1/2,j}^x = -(\overline{K}_1)_{i+1/2,j} \frac{p_{i+1,j} - p_{i,j}}{\Delta x_{i+1/2}}, \quad (3.10)$$

where  $(\overline{K}_1)_{i+1/2,j} = ((K_1)_{i+1/2,j^+} + (K_1)_{i+1/2,j^-})/2$ . The same argument can be used to show that

$$u_{i,j+1/2}^y = -(\overline{K}_2)_{i,j+1/2} \frac{p_{i,j+1} - p_{i,j}}{\Delta y_{j+1/2}}. \quad (3.11)$$

Finally, the boundary conditions also agree. Because of the artifice

$$(\overline{K}_1)_{1/2,j} = (\overline{K}_1)_{n_x+1/2,j} = (\overline{K}_2)_{i,1/2} = (\overline{K}_2)_{i,n_y+1/2} = 0$$

in the cell-centered method, (3.10) and (3.11) imply that  $u_h \cdot \nu = 0$ , which is the condition imposed in the space  $V_h$  in the mixed method.

The above results in (3.2), (3.10), and (3.11) can be summarized as follows.

**Theorem 2.** *The mixed method (2.1) can be written as the following cell-centered method:*

$$\begin{aligned} & -\frac{1}{\Delta x_i} \left( (\overline{K}_1)_{i+1/2,j} \frac{p_{i+1,j} - p_{i,j}}{\Delta x_{i+1/2}} - (\overline{K}_1)_{i-1/2,j} \frac{p_{i,j} - p_{i-1,j}}{\Delta x_{i-1/2}} \right) \\ & -\frac{1}{\Delta y_j} \left( (\overline{K}_2)_{i,j+1/2} \frac{p_{i,j+1} - p_{i,j}}{\Delta y_{j+1/2}} - (\overline{K}_2)_{i,j-1/2} \frac{p_{i,j} - p_{i,j-1}}{\Delta y_{j-1/2}} \right) \\ & = f_{ij}, \quad i = 1, \dots, n_x, \quad j = 1, \dots, n_y. \end{aligned}$$

### 4. Convergence and Superconvergence Results

Since the cell-centered finite difference methods arising from the Brezzi-Douglas-Marini (or Brezzi-Douglas-Durán-Fortin) and Raviart-Thomas-Nédélec mixed methods have the same form, the convergence and superconvergence results obtained for the latter method in [20] are also valid for the former method. Before stating the results, we need the following definition [2]. An asymptotic family of grids is said to be generated by a  $C^2$ -map if each grid is an image by a fixed map of a grid that is uniform in each coordinate direction. Let  $\|\cdot\|$  denote the  $L^2(\Omega)$ -norm, and  $\|\cdot\|_M$  be the norm induced by the inner product  $(\cdot, \cdot)_M$ . Let  $P_h$  be the  $L^2$ -projection onto  $W_h$ , and set  $h = \max_{ij} \{\Delta x_i, \Delta y_j\}$ .

**Theorem 3.** *There is a constant  $C$ , independent of  $h$ , such that*

$$\|\nabla \cdot (u - u_h)\| \leq Ch,$$

and, if  $p \in C^{3,1}(\bar{\Omega})$ ,  $u \in (C^1(\bar{\Omega}) \cap W^{2,\infty}(\bar{\Omega}))^d$ , and  $K \in (C^1(\bar{\Omega}) \cap W^{2,\infty}(\bar{\Omega}))^{d \times d}$ , then

$$\begin{aligned} \|P_h p - p_h\| &\leq Ch^2, \\ \|u - u_h\|_{TM} &\leq Ch^\alpha, \end{aligned} \tag{4.1}$$

where  $\alpha = 2$  if the grids are generated by a  $C^2$ -map or  $K$  is diagonal, and  $\alpha = 1$  otherwise.

The result (4.1) implies superconvergence for the computed pressure at the Gauss points (i.e., the centers of the elements).

### 5. An Expanded Mixed Formulation

We now consider the case where the permeability  $K$  can be zero in a subdomain of  $\Omega$ . The standard mixed formulation (1.2) requires inverting  $K$ , an impossibility in this degenerate case. Following [9, 10, 11], we consider the following expanded mixed formulation for (1.1): Find  $(u, \tilde{u}, p) \in V \times L^2(\Omega) \times W$  such that

$$\begin{aligned} (\nabla \cdot u, q) &= (f, q), & \forall q \in W, \\ (\tilde{u}, v) - (p, \nabla \cdot v) &= 0, & \forall v \in V, \\ (u, \tilde{v}) - (K\tilde{u}, \tilde{v}) &= 0, & \forall v \in L^2(\Omega). \end{aligned} \tag{5.1}$$

Corresponding to (2.1), the mixed finite element approximation of (5.1) is defined as follows: Find  $(u_h, \tilde{u}_h, p_h) \in V_h \times V_h \times W_h$  such that

$$\begin{aligned} (\nabla \cdot u_h, q) &= (f, q)_T, & \forall q \in W_h, \\ (\tilde{u}_h, v)_M - (p_h, \nabla \cdot v) &= 0, & \forall v \in V_h, \\ (u_h, \tilde{v})_M - (K\tilde{u}_h, \tilde{v})_M &= 0, & \forall v \in V_h, \end{aligned} \tag{5.2}$$

where  $V_h \times W_h$  is defined as before. Solvability of (5.2) can be shown as in Lemma 1.

From the second equation of (5.2), we express  $\tilde{u}_h$  in terms of  $p_h$  as in (3.10) and (3.11). This corresponds to a finite difference approximation of the equation  $\tilde{u} = -\nabla p$ . Then, from the third equation of (5.2), we express  $u_h$  in terms of  $\tilde{u}_h$ . This gives a finite difference approximation for the equation  $u = K\tilde{u}$ . Finally, substitute the second and third equations of (5.2) into the first equation of (5.1) to obtain a finite difference stencil for the pressure, which has the same form as in Theorem 2. Also, the error estimates in Theorem 3 hold for the expanded mixed finite element method [2].

### 6. Applications to Nonisothermal Multiphase Flow

The basic equations for nonisothermal multiphase, multicomponent flow and transport in a porous medium  $\Omega$  involve mass conservation, Darcy’s laws, energy conservation, and mole

fraction, saturation, and capillary pressure constraint equations. These equations are based on the displacement mechanisms of thermal methods: (a) reduction of crude viscosity with increasing temperature, (b) change of relative permeabilities for greater oil displacement, (c) vaporization of connate water and of portion of crudes for a miscible displacement of light components, and (d) high temperatures of fluids and rock to maintain high reservoir pressure. They can model the important physical factors and processes:

- viscosity, gravity, and capillary forces,
- heat conduction and convection processes,
- heat losses to overburden and underburden of a reservoir,
- mass transfer between phases,
- effects of temperature on physical property parameters of oil, gas, and water,
- rock compression and expansion.

We assume that the chemical components form at most three phases (e.g., water, oil, and gas), there are  $N_c$  chemical components that may exist in all three phases, and the diffusive effects are neglected.

Let  $\phi$  and  $k$  denote the porosity and permeability of the porous medium  $\Omega \subset \mathbb{R}^3$ , and  $S_\alpha$ ,  $\mu_\alpha$ ,  $p_\alpha$ ,  $u_\alpha$ , and  $k_{r\alpha}$  be the saturation, viscosity, pressure, volumetric velocity, and relative permeability of the  $\alpha$  phase,  $\alpha = w, o, g$ , respectively. Also, let  $\xi_{i\alpha}$  represent the molar density of component  $i$  in the  $\alpha$  phase,  $i = 1, 2, \dots, N_c$ ,  $\alpha = w, o, g$ . The molar density of phase  $\alpha$  is given by

$$\xi_\alpha = \sum_{i=1}^{N_c} \xi_{i\alpha}, \quad \alpha = w, o, g. \quad (6.1)$$

The mole fraction of component  $i$  in phase  $\alpha$  is then defined by

$$x_{i\alpha} = \xi_{i\alpha}/\xi_\alpha, \quad 1, 2, \dots, N_c, \quad \alpha = w, o, g. \quad (6.2)$$

The total mass is conserved for each component [14]:

$$\begin{aligned} \frac{\partial}{\partial t} \sum_{\alpha=w}^g x_{i\alpha} \xi_\alpha S_\alpha + \nabla \cdot \sum_{\alpha=w}^g x_{i\alpha} \xi_\alpha u_\alpha \\ = \sum_{\alpha=w}^g x_{i\alpha} q_\alpha, \quad i = 1, \dots, N_c, \end{aligned} \quad (6.3)$$

where  $q_\alpha$  stands for the flow rate of phase  $\alpha$  at wells. In equation (6.3), the volumetric velocity  $u_\alpha$  is given by Darcy's law:

$$u_\alpha = -\frac{k_{r\alpha}}{\mu_\alpha} k (\nabla p_\alpha - \rho_\alpha \wp \nabla z), \quad \alpha = w, o, g, \quad (6.4)$$

where  $\rho_\alpha$  is the mass density of the  $\alpha$ -phase,  $\wp$  is the magnitude of the gravitational acceleration, and  $z$  is the depth. The energy conservation equation takes the form

$$\begin{aligned} \frac{\partial}{\partial t} \left( \phi \sum_{\alpha=w}^g \rho_\alpha S_\alpha U_\alpha + (1 - \phi) \rho_s C_s T \right) \\ + \nabla \cdot \sum_{\alpha=w}^g \rho_\alpha u_\alpha H_\alpha - \nabla \cdot (k_T \nabla T) = q_c - q_L, \end{aligned} \quad (6.5)$$

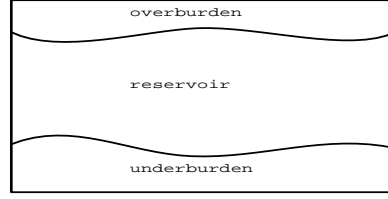


Fig. 1. Reservoir, overburden, and underburden.

where  $T$  is temperature,  $U_\alpha$  and  $H_\alpha$  are the specific internal energy and enthalpy of the  $\alpha$ -phase (per unit mass),  $\rho_s$  and  $C_s$  are the density and the specific heat capacity of the solid,  $k_T$  represents the total thermal conductivity,  $q_c$  denotes the heat source item, and  $q_L$  indicates the heat loss to overburden and underburden. In (6.5), the specific internal energy  $U_\alpha$  and enthalpy  $H_\alpha$  of phase  $\alpha$  can be computed as follows:

$$U_\alpha = C_{V\alpha}T, \quad H_\alpha = C_{p\alpha}T,$$

where  $C_{V\alpha}$  and  $C_{p\alpha}$  represent the heat capacities of phase  $\alpha$  at constant volume and pressure, respectively.

In addition to the differential equations (6.3)–(6.5), there are also algebraic constraints. The mole fraction balance implies

$$\sum_{i=1}^{N_c} x_{i\alpha} = 1, \quad \alpha = w, o, g. \quad (6.6)$$

In the transport process, the saturation constraint reads

$$S_w + S_o + S_g = 1. \quad (6.7)$$

Finally, the phase pressures are related by capillary pressures

$$p_{cow} = p_o - p_w, \quad p_{cgo} = p_g - p_o. \quad (6.8)$$

The equilibrium relations describing the distribution of hydrocarbon components into the phases are given by

$$\begin{aligned} f_{iw}(p_w, T, x_{1w}, x_{2w}, \dots, x_{N_cw}) &= f_{io}(p_o, T, x_{1o}, x_{2o}, \dots, x_{N_co}), \\ f_{io}(p_o, T, x_{1o}, x_{2o}, \dots, x_{N_co}) &= f_{ig}(p_g, T, x_{1g}, x_{2g}, \dots, x_{N_cg}), \end{aligned} \quad (6.9)$$

where  $f_{i\alpha}$  is the fugacity function of the  $i$ th component in the  $\alpha$  phase,  $i = 1, 2, \dots, N_c$ ,  $\alpha = w, o, g$ .

In thermal methods, heat is lost to the adjacent strata of a reservoir or the overburden and underburden, which is included in  $q_L$  of (6.5). We assume that the overburden and underburden extend to infinity along both the positive and negative  $x_3$ -axis (the vertical direction); see Fig. 1. If the overburden and underburden are impermeable, heat is entirely transferred through conduction. With all fluid velocities and convective fluxes being zero, the energy conservation equation (6.5) reduces to

$$\frac{\partial}{\partial t} (\rho_{ob} C_{p,ob} T_{ob}) = \nabla \cdot (k_{ob} \nabla T_{ob}), \quad (6.10)$$

where the subscript  $ob$  indicates that the variables are associated with the overburden and  $C_{p,ob}$  is the heat capacity at constant pressure. The initial condition is the original temperature  $T_{ob,0}$  of the overburden:

$$T_{ob}(x, 0) = T_{ob,0}(x).$$

The boundary condition at  $x_3 = 0$  (the top of the reservoir) is

$$T_{ob}(x_1, x_2, 0, t) = T(x_1, x_2, 0, t).$$

At infinity,  $T_{ob}$  is fixed:

$$T_{ob}(x_1, x_2, \infty, t) = T_\infty.$$

On other boundaries, we can use the impervious boundary condition

$$k_{ob}\nabla T_{ob} \cdot \boldsymbol{\nu} = 0,$$

where  $\boldsymbol{\nu}$  represents the outward unit normal to these boundaries. Now, the rate of heat loss to the overburden can be calculated by  $k_{ob}\nabla T_{ob} \cdot \boldsymbol{\nu}$ , where  $\boldsymbol{\nu}$  is the unit normal to the interface between the overburden and reservoir (pointing to the overburden). For the underburden, the heat conduction equation is given by

$$\frac{\partial}{\partial t}(\rho_{ub}C_{p,ub}T_{ub}) = \nabla \cdot (k_{ub}\nabla T_{ub}), \quad (6.11)$$

and similar initial and boundary conditions can be developed as for the overburden.

Equations (6.3)–(6.9) provide  $3N_c + 10$  independent relations, differential or algebraic, for the  $3N_c + 10$  dependent variables:  $x_{i\alpha}$ ,  $u_\alpha$ ,  $p_\alpha$ ,  $T$ , and  $S_\alpha$ ,  $\alpha = w, o, g$ ,  $i = 1, 2, \dots, N_c$ . If equations (6.10) and (6.11) are included, two more unknowns  $T_{ob}$  and  $T_{ub}$  are added. With proper initial and boundary conditions, there is a closed differential system for these unknowns. The mixed finite element methods implemented as finite differences are applied for the discretization of the governing equations. In time, a fully implicit scheme is exploited.

## 7. Numerical Experiments

The experimental problems are chosen from the benchmark problems of the fourth CSP [4]. Six companies participated in that comparison project. Two related steam injection problems were numerically studied. The first problem deals with cyclic steam injection in a non-distillable petroleum reservoir with two-dimensional radial cross-sectional grids, and the second problem deals with non-distillable oil displacement by steam in an inverted nine-spot pattern by considering one-eighth of the full pattern (see Fig. 2). Standard conditions for these problems are 14.7 psia and 60°F. The problems were chosen to exercise features of the models that are important in practical applications, though they may not represent a real field analysis.

Table 1. Rock properties.

|  |
|--|
| $k_h$ starting with the top layer: 2,000, 500, 1,000, and 2,000 md |
| $k_v$ : 50% of $k_h$   |
| Porosity: 0.3 for all layers                                       |
| Thermal conductivity: 24 BTU/(ft.-day-°F)                          |
| Heat capacity: 35 BTU/(ft <sup>3</sup> of rock-°F)                 |
| Effective rock compressibility: 5.0E-4 psi <sup>-1</sup>           |

Table 2. Oil properties.

|  |
|--|
| Density at standard conditions: 60.68 lb/ft <sup>3</sup> |
| Compressibility: 5.0E-6 psi <sup>-1</sup>                |
| Molecular weight: 600                                    |
| Thermal expansion coefficient: 3.8E-4 1/°R               |
| Specific heat: 0.5 BTU/(lb.-°R)                          |

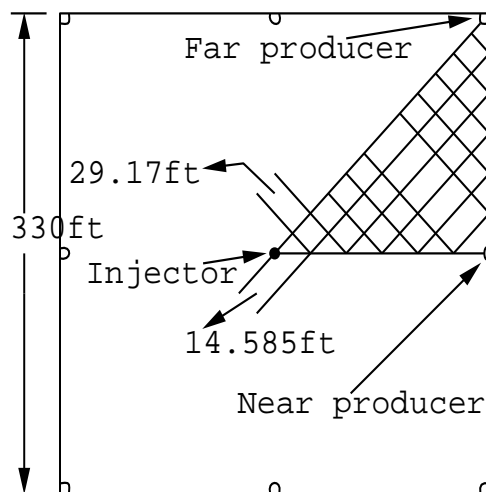


Fig. 2. Element of symmetry in an inverted nine-spot.

### 7.1. The First Problem

The aim is to simulate cyclic steam injection in a two-dimensional reservoir (closed system) that has four layers. The rock properties are stated in Table 1, where  $k_h$  and  $k_v$  denote the horizontal and vertical permeabilities, respectively, and the thermal conductivity and heat capacity are for the reservoir, overburden, and underburden. Water is assumed to be pure water with standard properties. Oil properties are listed in Table 2, and the viscosity dependence on temperature is given in Table 3. The capillary pressures are zero. The initial conditions are presented in Table 4, where the pressure distribution is according to the gravity head.

Table 3. Oil viscosity dependence on temperature.

| Temp ( $^{\circ}$ F) | 75    | 100   | 150 | 200 | 250  | 300 | 350 | 500 |
|----------------------|-------|-------|-----|-----|------|-----|-----|-----|
| Viscosity (cp)       | 5,780 | 1,389 | 187 | 47  | 17.4 | 8.5 | 5.2 | 2.5 |

Table 4. Initial conditions.

|  |
|--|
| Oil saturation: 0.55                             |
| Water saturation: 0.45                           |
| Reservoir temperature: 125 $^{\circ}$ F          |
| Pressure at the center of the top layer: 75 psia |

The computational grid uses a cylindrical grid with 13 grid points in the radial direction. The well radius is 0.3 ft, and the exterior radius is 263.0 ft. The block boundaries in the radial direction are at 0.30, 3.0, 13.0, 23.0, 33.0, 43.0, 53.0, 63.0, 73.0, 83.0, 93.0, 103.0, 143.0, and 263.0 ft, and the block boundaries in the vertical direction are at 0.0 (top of pay), 10.0, 30.0, 55.0, and 80.0 ft. The depth to the top of pay is 1,500 ft subsea.

Finally, the operating conditions are summarized as follows: All layers are open to flow during injection and production (zero skin factor). The energy content of the injected steam is based on 0.7 quality and 450 $^{\circ}$ F. Steam quality at bottom hole conditions is fixed at 0.7. Three cycles are simulated: Each cycle is of 365 days with injection for 10 days followed by a 7 day soak period, and the cycle is completed with 348 days of production. Steam is injected at capacity subject to the following conditions: The maximum bottom-hole pressure is 1,000 psia at the center of the top layer, and the maximum injection rate is 1,000 STB/day. The production capacity is subject to the following constraints: The minimum bottom-hole pressure is 17 psia at the center of the top layer, and the maximum production rate is 1,000 STB/day of liquids.

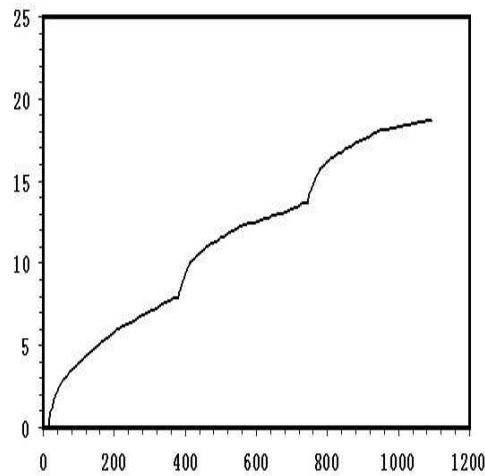


Fig. 3. Cumulative oil production (MSTB) vs. time (days).

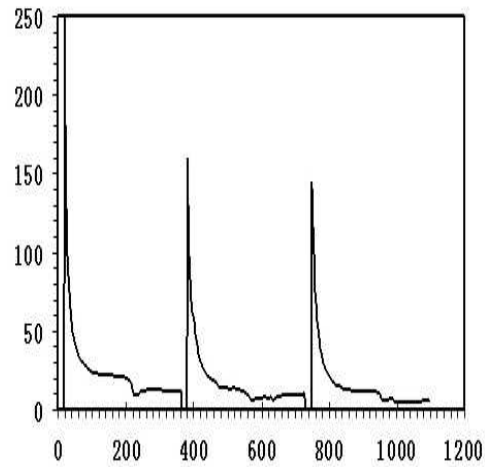


Fig. 4. Oil production rate (STB/day).

Figs. 3 and 4 show the cumulative oil production and oil production rate, respectively. Compared with the results presented in [4], the two quantities in Figs. 3 and 4 are close to the respective averaged values of those provided by the six companies for the first problem.

## 7.2. The Second Problem

The objective is to simulate one-eighth of an inverted nine-spot pattern via symmetry. The total pattern area is 2.5 acres. The rock and fluid properties, relative permeability data, and initial conditions are the same as those for the first problem. The grid dimensions are  $9 \times 5 \times 4$  (uniform in the horizontal direction). The radius of all wells is 0.3 ft.

The operating conditions are given as follows: Injection occurs only in the bottom layer, and production occurs from all four layers. Steam conditions are the same as in the first problem. Steam is injected at capacity subject to the following conditions: The maximum bottom-hole pressure is 1,000 psia at the center of the bottom layer, and the maximum injection rate is 1,000 STB/day on a full-well basis. The production capacity is subject to the following constraints: The minimum bottom-hole pressure is 17 psia at the center of the top layer, the maximum

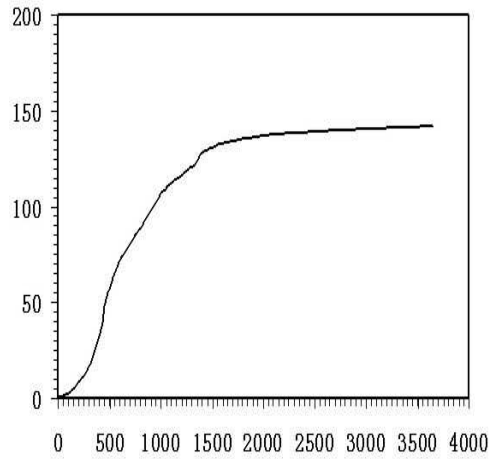


Fig. 5. Cumulative oil production for the full pattern (MSTB vs. days).

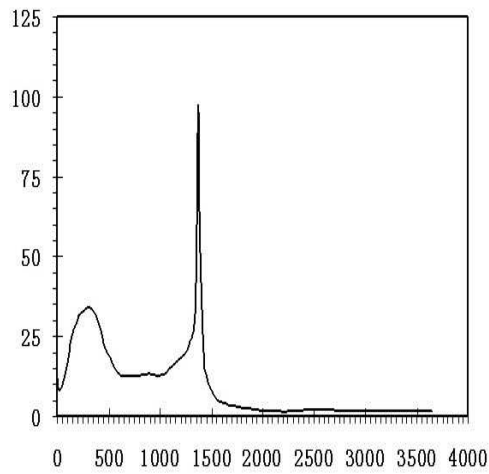


Fig. 6. Oil production rate for the far producer (STB/day).

production rate is 1,000 STB/day of liquids, and the maximum steam rate is 10 STB/day. The simulation time is 10 years of injection and production.

Figs. 5–7 indicate the cumulative oil production for the full pattern, the oil production rate for the far producer, and the oil production rate for the near producer, respectively. All well data presented are on a full-well basis, and the pattern results are for the full pattern consisting of four quarter (far) producers and four half (near) producers. Again, compared with the results presented in [4], the three quantities are close to the respective averaged values of those provided by the six companies for the second problem.

## References

- [1] T. Arbogast and Z. Chen, On the implementation of mixed methods as nonconforming methods for second order elliptic problems, *Math. Comp.*, **64** (1995), 943–972.
- [2] T. Arbogast, M. F. Wheeler and I. Yotov, Mixed finite elements for elliptic problems with tensor coefficients as cell-centered finite differences, *SIAM J. Numer. Anal.*, **34** (1997), 828–852.

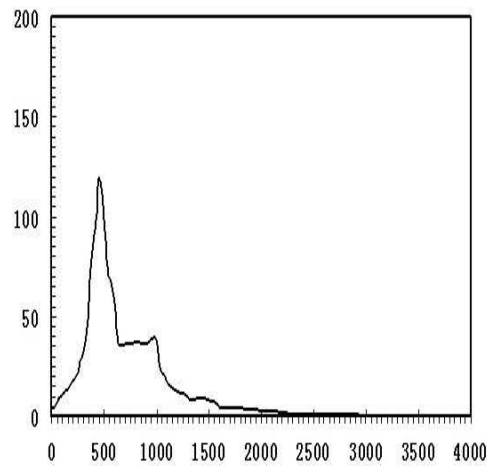


Fig. 7. Oil production rate for the near producer (STB/day).

- [3] D. Arnold and F. Brezzi, Mixed and nonconforming finite element methods: implementation, postprocessing and error estimates, *RAIRO Modél. Math. Anal. Numér.* **19** (1985), 7–32.
- [4] Aziz, K., B. Ramesh, and P. T. Woo, Fourth SPE comparative solution project: A comparison of steam injection simulators, SPE 13510, SPE Reservoir Simulation Symposium Dallas, Texas, February 10–13, 1985, pp. 441–454.
- [5] F. Brezzi, J. Douglas, Jr., R. Durán and M. Fortin, Mixed finite elements for second order elliptic problems in three variables, *Numer. Math.*, **51** (1987), 237–250.
- [6] F. Brezzi, J. Douglas, Jr., M. Fortin, and L. Marini, Efficient rectangular mixed finite elements in two and three space variables, *RAIRO Modél. Math. Anal. Numér.*, **21** (1987), 581–604.
- [7] F. Brezzi, J. Douglas, Jr., and L. Marini, Two families of mixed finite elements for second order elliptic problems, *Numer. Math.*, **47** (1985), 217–235.
- [8] Z. Chen, Analysis of mixed methods using conforming and nonconforming finite element methods, *RAIRO Modél. Math. Anal. Numér.*, **27** (1993), 9–34.
- [9] Z. Chen, BDM mixed methods for a nonlinear elliptic problem, *J. Comp. Appl. Math.*, **53** (1994), 207–223.
- [10] Z. Chen, Expanded mixed finite element methods for linear second order elliptic problems I, *RAIRO Model. Math. Anal. Numer.*, **32** (1998), 479–499.
- [11] Z. Chen, Expanded mixed finite element methods for quasilinear second order elliptic problems II, *RAIRO Model. Math. Anal. Numer.*, **32** (1998), 501–520.
- [12] Z. Chen, Equivalence between and multigrid algorithms for nonconforming and mixed methods for second order elliptic problems, *East-West J. Numer. Math.*, **4** (1996), 1–33.
- [13] Z. Chen and J. Douglas, Jr., Prismatic mixed finite elements for second order elliptic problems, *Calcolo*, **26** (1989), 135–148.
- [14] Z. Chen, G. Huan and Y. Ma, Computational Methods for Multiphase Flows in Porous Media, in the Computational Science and Engineering Series, Vol. 2, SIAM, Philadelphia, PA, 2006.
- [15] L. D. Marini, An inexpensive method for the evaluation of the solution of the lowest order Raviart-Thomas mixed method, *SIAM J. Numer. Anal.*, **22** (1985), 493–496.
- [16] J. C. Nédélec, Mixed finite elements in  $\mathbf{R}^3$ , *Numer. Math.*, **35** (1980), 315–341.
- [17] J. C. Nédélec, A new family of mixed finite elements in  $\mathbf{R}^3$  *Numer. Math.*, **50** (1986), 57–81.
- [18] P. A. Raviart and J. M. Thomas, A mixed finite element method for 2nd order elliptic problems, *Mathematical Aspects of the Finite Element Method*, Lecture Notes in Mathematics 606, Springer-Verlag, Berlin, 1977, 292–315.

- [19] T. Russell and M. F. Wheeler, Finite element and finite difference methods for continuous flows in porous media, Chapter II, *The Mathematics of Reservoir Simulation*, R. Ewing, ed., *Frontiers in Applied Mathematics 1*, Society for Industrial and Applied Mathematics, Philadelphia, 1983, 35–106.
- [20] A. Weiser and M. F. Wheeler, On convergence of block-centered finite-differences for elliptic problems, *SIAM J. Numer. Anal.*, **25** (1988), 351–375.